aerospace

MDPI

Article

Optimization Design of Core Ultra-Stable Structure for Space Gravitational Wave Detection Satellite Based on Response Surface Methodology

Changru Liu [1,2], Zhenbang Xu [1,2,*], Kang Han [1], Chengshan Han [1,2] and Tao He [3]

[1] Changchun Institute of Optics, Fine Mechanicsand Physics, Chinese Academy of Sciences, Changchun 130022, China; liuchangru@ciomp.ac.cn (C.L.); han_chengshan@163.com (C.H.)
[2] School of Materials Science and Optoelectronic Technology, University of Chinese Academy of Sciences, Beijing 100049, China
[3] Innovation Academy for Microsatellites of Chinese Academy of Sciences, Shanghai 200003, China; hetao@microsate.com
* Correspondence: xuzhenbang@ciomp.ac.cn

Abstract: In order to meet the urgent demand for novel zero-expansion materials and ultra-stable structures in space gravitational wave detection, it is necessary to develop an ultra-stable structural spacecraft system. This paper focuses on the research of the optimization of the core ultra-stable structure design of spacecraft, proposing a cross-scale parameterized model of structural deformation response and a multi-objective optimization method. By satisfying the prerequisites of mass and fundamental frequency, this paper breaks through the limitations of current linear analysis methods, and the overall thermal deformation of nonlinear material composite structures is optimized by modifying structural parameters.

Keywords: space gravitational wave detection; ultra-stable structure; ultra-low thermal deformation; multi-objective optimization; response surface methodology; C/SiC box structure

Citation: Liu, C.; Xu, Z.; Han, K.; Han, C.; He, T. Optimization Design of Core Ultra-Stable Structure for Space Gravitational Wave Detection Satellite Based on Response Surface Methodology. *Aerospace* **2024**, *11*, 518. https://doi.org/10.3390/aerospace11070518

Academic Editor: Hyun-Ung Oh

Received: 15 May 2024
Revised: 20 June 2024
Accepted: 24 June 2024
Published: 26 June 2024

1. Introduction

In response to the spatiotemporal scale characteristics of gravitational wave detection, this study aims to reveal the deformation response mechanisms and transmission laws of ultra-stable structures under thermal loading. Based on multi-level substructures and interface continuity conditions, a cross-scale networked parameter model of material–process–structure for ultra-stable structures is established. This model elucidates the mapping relationship between structural parameter domains and deformation responses. With the objectives of minimizing deformation responses and maximizing overall stiffness, structural parameter network optimization is pursued to achieve a complete layout and configuration design of ultra-stable structures.

Space gravitational wave detection satellites are ultra-quiet and ultra-stable spacecraft with high technical specifications, complex systems, and significant implementation challenges [1]. The stability of structural dimensions is one of the most critical aspects of such satellites, posing a major question regarding the choice of support structures for the satellite and its core scientific payloads. Laser interferometric space gravitational wave detection based on ultra-long baselines aims to achieve ultra-high-precision measurements of strain in the frequency range from mHz to Hz, reaching magnitudes of 10^{-20} to 10^{-22}. However, this ambitious goal faces enormous challenges, including picometer-level optical path noise and residual acceleration noise of 10^{-15} m/s^2. Thermal deformation noise typically affects gravitational wave detection in frequency bands ranging from 1 mHz to 0.1 Hz, including picometer-level thermal optical path noise across the entire chain and spacecraft thermal-inducing self-gravity noise at the level of 10^{-16} m/s^2. To address these two core

challenges, high-precision temperature control of the satellite is required (with core component temperatures stable at the level of 10 μK) while employing ultra-low-expansion material systems or even zero-expansion materials (with thermal expansion coefficients <1 × 10^{-7}/K) for construction [2].

The main approaches to achieving low-thermal-expansion materials and structures, both domestically and abroad, can be categorized into four types: homogeneous materials, lattice-based metamaterials, positive–negative structure assembly, and composite materials. The coefficient of thermal expansion for metallic materials, even for super Invar alloys, is as low as 3.1 × 10^{-7}/K. Super Invar alloys are commonly used in the structural and optical components of space telescopes and sensors, where high precision and thermal dimensional stability are critical requirements. The thermal expansion of Invar can be reduced through partial substitution of Ni by Co. Some high-performance detectors, such as infrared sensors and bolometers, require a cryogenic environment to avoid thermal noise. This alloy is known as super Invar. These alloys are being tested as telescope components for the Small JASMINE satellite, Thirty Meter Telescope (TMT), and other applications. However, super Invar alloys have high density and magnetism, making them unsuitable for the core structures of gravitational wave detectors [3]. Inorganic materials such as ZERODUR can achieve a thermal expansion coefficient of 1.5 × 10^{-8}/K. ZERODUR, positioned between glass and crystal, is a highly isotropic homogeneous material with very low levels of bubbles, inclusions, striation defects, and stress. Due to its transparency in visible light, it can be thoroughly inspected to eliminate any unexpected occurrences during the manufacturing process. ZERODUR is widely used in astronomy. Prominent telescopes have operated ZERODUR mirror substrates for several decades [4]. Examples are the earth-bound segmented telescopes Keck I (28 years) and II (25 years), Grantecan (14 years), HET (25 years), and Lamost (13 years); the telescopes with the largest monolithic cast mirrors ESO VLT (23 years); and the space-borne X-ray telescope Chandra (22 years) However, due to poor thermal conductivity, high brittleness, and poor machinability, it cannot be used for large-sized complex load-bearing structures. The University of Michigan has achieved cobalt alloy planar lattice composite materials with a thermal expansion coefficient of 1 × 10^{-6}/K in the laboratory. However, the preparation process is prone to thermal stress fracture and is only suitable for small-sized planar components, with no reported applications in satellites. The University of Florida has developed a single leg (0.11 m long) with a thermal expansion coefficient of 6 × 10^{-7}/K by joining negative thermal expansion ALLVAR alloy with titanium alloy. However, factors such as assembly and adjustment affect the thermal expansion coefficient of the hexapod assembly, deteriorating to 3.9 × 10^{-6}/K.

Currently, space optical support structures mainly exist in two forms: truss and frame. Truss structures are highly lightweight but have disadvantages in terms of integrity and stability; they are more sensitive to structural dimensional changes and pose stability risks. A typical example of a space camera truss support structure is the Hubble Space Telescope (HST), which has a diameter of approximately 2.4 m and a length of 4.9 m and is composed of 48 rods made from graphite fiber-reinforced epoxy composite materials. This structure exhibits good thermal stability. The ALOS-3 satellite developed by the Japan Aerospace Exploration Agency (JAXA) was launched in 2021, featuring a camera with an off-axis optical system that uses a lightweight truss structure for its main support. Frame support structures, on the other hand, offer excellent integrity, high stability, and simple assembly processes. They are well-suited for achieving the high rigidity and stability required for gravitational wave structures. Scholars, both domestically and internationally, have conducted extensive research on frame support structures. The Advanced Land Imager (ALI) onboard the EO-1 Earth observation satellite, launched by the United States in 2000, utilizes a frame support structure. Similarly, the Gaofen-6 satellite, successfully launched by China in 2018, employs a thin-wall frame architecture, marking the largest application of high-volume aluminum-based composites in Chinese space cameras to date [5]. Structural optimization design can be broadly categorized into three types: size optimization, shape

optimization, and topology optimization. Topology optimization is a core design method during the initial design phase. It fundamentally designs the topology of the structure by reasonably distributing materials according to optimization objectives, and it falls under conceptual design. Compared to empirical manual designs, topology optimization yields more innovative configurations with superior performance while providing designers with broader design ideas and expanding the design space. Shape optimization and size optimization, on the other hand, focus more on detailed design aspects, often targeting hole shapes, rod cross-sectional sizes, plate shell thicknesses, and similar features for optimization [6].

C/SiC is a ceramic matrix composite reinforced with continuous carbon fibers. It exhibits extremely high thermal stability and environmental stability in humid conditions, with a typical coefficient of thermal expansion around 1×10^{-6}/K. Through the optimization of fiber/matrix selection, Northwestern Polytechnical University has achieved a material-level coefficient of thermal expansion of 1.0×10^{-7}/K [7–9]. This material has been applied in the research of the Taiji-II mission. Simultaneously, the development of a φ1260 mm × 1580 mm space camera mirror barrel was realized at the 10^{-6}/K level. C/SiC is considered one of the most promising materials for achieving zero-expansion performance and large-size ultra-stable structures due to its ultra-high stability and high toughness [10]. However, the structural system of gravitational-wave space missions is complex, with significant interface coupling and diverse characteristics in terms of dimensions, functions, and manufacturing processes of structural components. Therefore, further research is needed on how to optimize the construction of spacecraft structural systems based on low-expansion material systems.

2. Design Requirements and Constraints for the Core Ultra-Stable Structure of Gravitational Wave Detection

According to the analysis of the spacecraft's ultra-stable structure system composition, the CUSS of the spacecraft is installed on the secondary ultra-stable structure satellite platform through trusses. It is divided into several parts, including the telescope, optical bench (OB), detection system, core ultra-stable system, secondary ultra-stable structure, and platform peripheral structure. The core ultra-stable system provides support for precision test structures such as inertial propagation, playing a crucial role in determining the accuracy of gravitational wave measurements.

Designing the ultra-stable framework within the CUSS and exploring structural size optimization schemes are imperative. On the one hand, the ultra-stable structure framework needs to support two sets of detection system structures, and on the other hand, it needs to maintain stable connections with the satellite platform. To mitigate the impact of temperature, self-gravity, and other factors on the precision of gravitational wave measurements, the ultra-stable structure framework is required to provide stable support for the measurement system structure, capable of resisting subtle deformations caused by self-gravity and thermal changes. Since ultra-stable spacecraft structures are intended for space application, stringent temperature requirements are necessary during usage. Therefore, the design of the ultra-stable framework also needs to consider factors such as operational temperature ranges and launch dynamics, demonstrating a certain level of temperature adaptability and resistance to mechanical forces.

Considering the extreme sensitivity of the core structure of gravitational wave detection to temperature deformation, the CUSS framework adopts C/SiC low-thermal-expansion composite materials. In the design process of the ultra-stable framework, this material's molding process needs to be considered as one of the constraints to ensure the subsequent framework's molding and processing performance [11]. Based on the application requirements of the CUSS and the characteristics of the material molding process, the CUSS framework needs to meet the following requirements:

(a) The core ultra-stable structural framework needs to provide stable support for two sets of detection system structures, with the outer diameter envelope size of the two

detection systems being φ450 mm (tentative) and the angle between them being 60°, with a tentative axial spacing of 618 mm;

(b) The core ultra-stable structural framework requires corresponding interfaces to achieve a stable connection with the satellite platform;

(c) The overall dimensions of the core ultra-stable structural framework are greater than 1200 mm × 1000 mm × 100 mm;

(d) The supported load mass ≥ 400 kg;

(e) Structural fundamental frequency ≥ 50 Hz;

(f) The weight of the core ultra-stable structural sample ≤ 70 kg;

(g) The equivalent coefficient of thermal expansion in two directions in the plane $\leq 1 \times 10^{-7}$/K.

3. Parametric Modeling of Core Ultra-Stable Structure

The requirements for space gravitational-wave spacecraft entail meeting the picometer-level optical path noise of the payload. Firstly, the direct connection structure of the payload needs to possess extremely stable dimensional stability, including a thermal expansion coefficient of less than 1×10^{-7}/K. On the one hand, the core ultra-stable structural framework connects to the core module panel of the platform, and on the other hand, it provides support for the interferometer, inertial sensors, and telescope connection mechanisms. Its dimensional stability directly influences the optical path noise, necessitating the structure itself to have a high strength-to-weight ratio, high stiffness-to-weight ratio, and resistance to mechanical vibrations during the launch phase. To reduce weight, the CUSS as a whole adopts a high-rigidity, thin-walled, lightweight frame structure. It needs to be able to resist the forces resulting from changes in the core module panel dimensions, ultimately providing a maximally stable observation environment for gravitational wave detection.

The main function of the core ultra-stable structural framework is to support two sets of detection system structures. To achieve support for the two sets of detection system structures, the ultra-stable structural framework can be divided and designed according to the different functions of each part, providing guidance for subsequent optimization. According to the requirements of gravitational wave detection for the core ultra-stable structural framework, the framework can be divided into supporting structures, central reinforcement beams, and auxiliary frame structures, as shown in Figure 1.

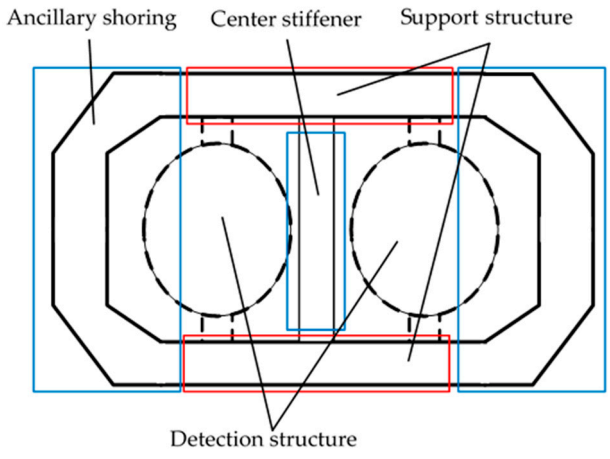

Figure 1. Division of the core support framework structure.

The support structure, central reinforcing beams, and auxiliary supports are all made of C/SiC composite materials and assembled into a box-type structure. The issue of unstable expansion coefficients caused by connections has been addressed through homogenous connection techniques. By utilizing the ultra-low-expansion coefficient of C/SiC composite materials, they are processed into pins and bolts and connected together using deposition processes. This allows for composite connections while avoiding a sharp increase in expansion coefficients at the connection site. To meet the overall rigidity of the framework,

reinforcement ribs are added at appropriate positions in the box structure, and the final framework model structure is shown in Figure 2. Two sets of detection system structures are located at the center of the holes on both sides of the framework.

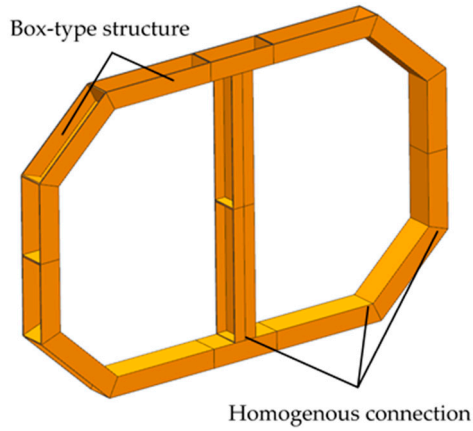

Figure 2. Model of the core support framework figure.

The core ultra-stable structural framework is supported on the satellite platform via trusses. When analyzing the CUSS, it is necessary to constrain the interface between the trusses and the satellite platform. The trusses are composed of negative thermal expansion carbon fiber composite materials and titanium alloy inserts, achieving zero expansion within the working temperature range through linear expansion matching. To facilitate the optimization and analysis of the core ultra-stable structural framework, the support structure of the framework is simplified. The support method of the CUSS is shown in Figure 3.

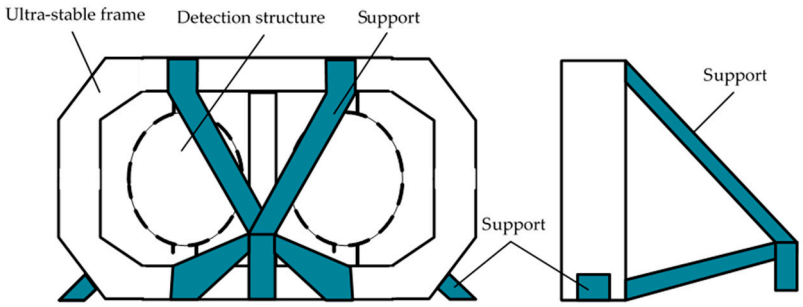

Figure 3. Core ultra-stable structural support method.

Once the CUSS form is determined, due to the anisotropic nature of C/SiC materials, in order to minimize overall linear expansion and achieve optimal mass while meeting launch mechanical requirements, it is necessary to optimize the dimensional parameters. Before conducting dimensional optimization, a parameterized model is established. During optimization, parameters are modified based on different algorithms, and corresponding output structures are calculated to achieve iterative computation. The dimensions and parameters of the CUSS are represented as shown in Figure 4.

The meanings and value ranges of each parameter are shown in Table 1. During iterative optimization, if the optimal solution requires parameters to reach the limits of their value range, the range can be further expanded as needed until the optimal solution is achieved within the overall range.

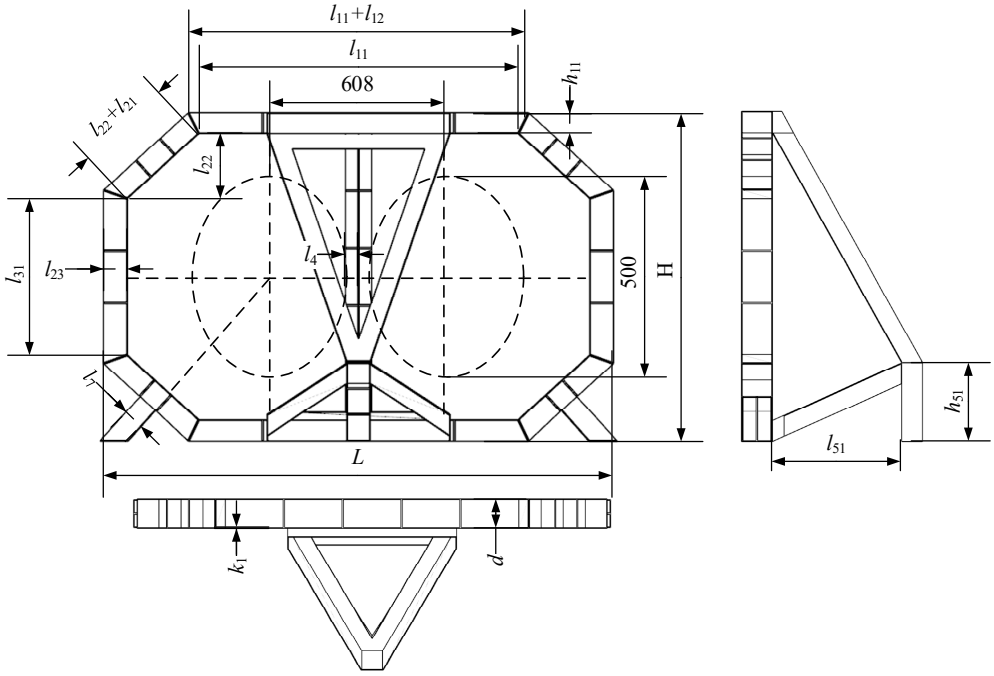

Figure 4. Parametric model of core super-stable framework.

Table 1. Range of parameter values.

Number	Parameter Name	Value Range (mm)	Number	Parameter Name	Value Range (mm)
1	Main Beam Short Side Length—l_{11}	700~1100	7	Vertical Beam Width—l_{23}	50~200
2	Main Beam Long Side Length—l_{12}	50~200	8	Vertical Beam Short Side Width—l_{31}	600~1000
3	Main Beam Height—h_{11}	100~200	9	Central Beam Thickness—l_4	20~129
4	Frame Thickness—d	100~300	10	Support Distance—l_{51}	200~600
5	Diagonal Beam Short Side Length—l_{21}	50~200	11	Support Height—h_{51}	200~700
6	Diagonal Beam Vertical Height—l_{22}	100~400	12	Structural Member Wall Thickness—k_1	2~5

4. Response Surface Method Parameter Optimization

The CUSS of the gravitational-wave spacecraft is complex, with ceramic-based silicon carbide composite materials exhibiting anisotropy and multiple factors influencing thermal deformation. Design-related empirical formulas are not yet available, making it difficult to obtain the optimal design solution using traditional empirical or trial-and-error methods [12]. To achieve the optimal stability of the CUSS of the gravitational-wave spacecraft, an optimization algorithm combined with the finite element method is employed to optimize the parameters of the core component integrated framework structure. The main objective is to achieve the optimal comprehensive performance of the core component integrated framework while meeting the design criteria.

4.1. Optimization Process Design

Firstly, target parameters for optimizing the core ultra-stable structural framework are selected based on the index requirements, and their value ranges are determined while also clarifying the interdependent conditions among structural parameters [13]. The methods for selecting experimental points include full factorial design, orthogonal array, central composite design, Box–Behnken design, Latin hypercube design, and optimal Latin hypercube design [14]. Among these, the Box–Behnken design consists of multiple orthogonal cubes and includes a central point. Because it avoids extreme points, it can be applied to the optimization of mechanical dimensions, preventing cases where a dimension is too small to conduct the experiment or where the results are unstable. The Box–Behnken design allows for accurate estimation of second-order effects while maintaining a sufficient number of experimental points. Therefore, we chose the Box–Behnken design method to select the experimental points required for response surface methodology (RSM) [15].

The finite element analysis software was used for iterative calculations in the simulation analysis of the core ultra-stable structure of the gravitational-wave spacecraft. During the iterative optimization process, automatic modeling and analysis were completed using ".ses" commands. The element type used was tetrahedral elements with a mesh size of 2 mm, and the constraint points were nodes in the plane formed by the three support corners. A temperature load of 1 K temperature rise was applied to the overall structure. The ceramic matrix C/SiC composite material is anisotropic [16]. Based on the ply orientation of the carbon fibers, local coordinate systems were established for each plane of the core ultra-stable framework structure of the gravitational-wave spacecraft, and material properties were assigned, as shown in Table 2. To simulate the load, the mirror assembly connected to the core ultra-stable structure was also modeled. After modeling, the total mass of the finite element model of the spacecraft's ultra-stable structure was 404.1 kg, with the frame assembly weighing 53.6 kg and the mirror assembly weighing 350.5 kg. Modal and static analyses were performed using the finite element analysis software to extract fundamental frequencies and deformation results [17]. Ultimately, the optimization equations were subsequently fitted. And the optimal design parameters are obtained. The optimization process for the CUSS of the gravitational-wave spacecraft is illustrated in Figure 5.

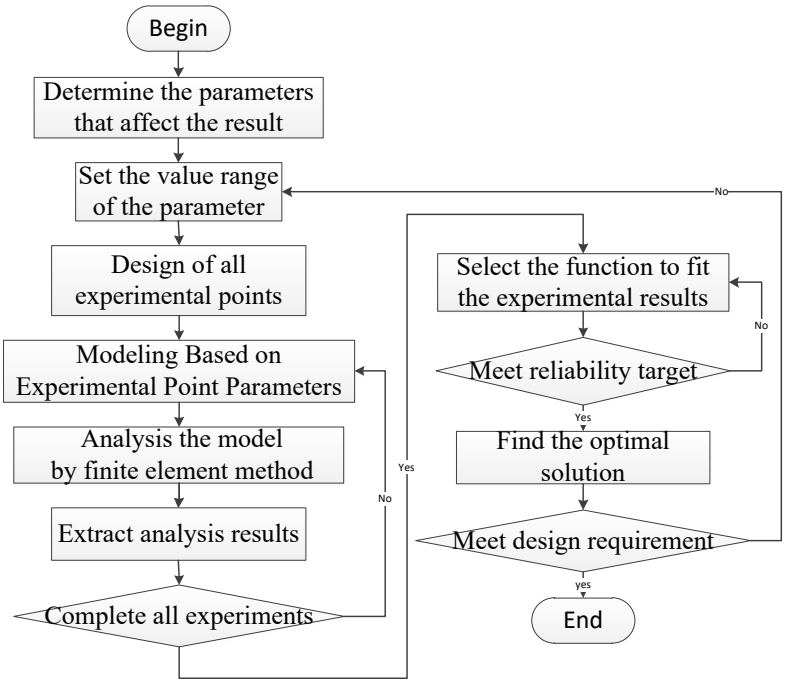

Figure 5. Flowchart of CUSS optimization process.

Table 2. Material properties of **C/SiC**.

Type	Tensile Strength (MPa)			Density (g/cm^3)	CET 10^{-7}/K		
	E_1	E_2	E_3		α_{11}	α_{22}	α_{33}
M55-C/SiC(Modified)	380	380	305	2.10	2.6	2.6	5.8

4.2. Parameter Constraint Conditions and Optimization Objectives

According to the structure in Figure 4, the total length of the CUSS is denoted as L.

$$\mathrm{L} = l_{11} + l_{22} + 2\sqrt{(l_{21} + l_{22})^2 - l_{22}^2} + 2l_{23}$$

The total height of the frame structure is denoted as H.

$$\mathrm{H} = l_{31} + 2l_{22} + 2h_{11}$$

The total thickness of the framework is denoted as D.

$$\mathrm{D} = d$$

To meet the requirement that the overall dimensions of the CUSS framework are greater than 1200 mm × 1000 mm × 100 mm.

$$\begin{cases} \mathrm{L} = l_{11} + l_{22} + 2\sqrt{(l_{21} + l_{22})^2 - l_{22}^2} + 2l_{23} \geq 1200 \\ \mathrm{H} = l_{31} + 2l_{22} + 2h_{11} \geq 1000 \\ \mathrm{D} = d \geq 100 \end{cases}$$

To meet the installation requirements of the detection system and allow a safety margin of 50 mm, it is required that each dimension satisfies the following:

$$\begin{cases} (608 - 500\sin 30^\circ)/2 - l_4 \geq 50 \\ (l_{11} + 2\sqrt{(l_{21} + l_{22})^2 - l_{22}^2} - 608 - 500\sin 30^\circ)/2 \geq 50 \\ l_{31}/2 + l_{22} - 500 \geq 50 \\ \sqrt{(\frac{l_{31}}{2} + l_{22})^2 + (\frac{l_{11}-608}{2})^2}\cos(90^\circ - \arccos(\frac{l_{22}}{l_{21}}) - arctan(\frac{(l_{11}-608)/2}{l_{31}/2+l_{22}})) - 250\sin(90^\circ - \arccos(\frac{l_{22}}{l_{21}})) \geq 50 \end{cases}$$

To meet the requirements of system mass and launch mechanics, the corresponding weight K and launch fundamental frequency M should satisfy the following:

$$\begin{cases} \mathrm{K} \geq 60\,\mathrm{kg} \\ \mathrm{M} \geq 40\,\mathrm{Hz} \end{cases}$$

The thermal expansivity in two directions within the plane of the core ultra-stable structural framework are denoted as α_L and α_H, with expressions given as follows:

$$\alpha_\mathrm{L} = \frac{\Delta l_\mathrm{L}}{\mathrm{L}\Delta T}, \alpha_\mathrm{H} = \frac{\Delta l_\mathrm{H}}{\mathrm{H}\Delta T}$$

where L and H represent the total length and total height of the frame, respectively; Δl_L and Δl_H denote the deformation caused by thermal expansion in two directions; and ΔT represents the temperature variation.

The design optimization objective is to minimize α_L and α_H to less than 1×10^{-7}/K.

$$\begin{cases} \text{minimize } \alpha_\mathrm{L} \\ \text{maximize } \alpha_\mathrm{H} \end{cases}$$

5. Optimization Results

Based on the parameters of each test point, a structural model of the core ultra-stable framework is established, and the finite element method is employed to calculate the equivalent thermal expansion coefficients α_L and α_H in the plane of the core ultra-stable platform, as well as the fundamental frequency K and mass M. Following the principles of response surface methodology, various fitting techniques including linear equations, quadratic polynomials, and two-factor interactions are compared for their effectiveness in fitting design parameters and results. Through this comparison, the mathematical expressions for α_L, α_H, K, and M are derived using quadratic polynomials to minimize errors.

The relationships between the deformation caused by thermal expansion in two directions, Δl_L and Δl_H, and the sensitive design parameters are shown in Figures 6 and 7, respectively. Among them, the equivalent thermal expansion coefficient α_L is sensitive to the height h_{11} of the main beam, the vertical height l_{22} of the diagonal beam, and the length l_{31} of the vertical beam; the equivalent thermal expansion coefficient α_H is sensitive to the height h_{11} of the main beam, the thickness d of the frame, the length l_{21} of the diagonal beam, the width l_{23} of the vertical beam, and the height l_{51} of the support; the fundamental frequency is sensitive to the length l_{11} of the main beam, the length l_{12} of the main beam, the thickness d of the frame, the vertical height l_{22} of the diagonal beam, the width l_{23} of the vertical beam, the length l_{31} of the vertical beam, and the distance l_{51} of the support; and the mass is sensitive to all dimensional parameters. The parameters l_{11}, l_{21}, l_{22}, l_{23}, l_{31}, l_4, h_{51}, and k_1 have a positive effect on the equivalent thermal expansion coefficient α_L, while the other parameters have a negative effect on the equivalent thermal expansion coefficient α_L; the parameters l_{12}, h_{11}, d, and l_{31} have a positive effect on the equivalent thermal expansion coefficient α_H, while the other parameters have a negative effect on the equivalent thermal expansion coefficient α_H.

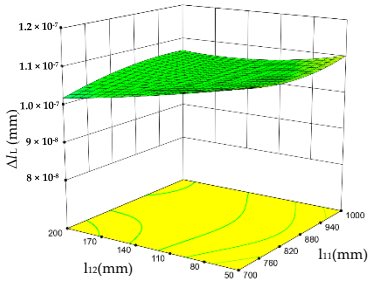

(**a**) Response surface relationship between structural deformation Δl_L and sensitive parameters l_{12} and l_{11}.

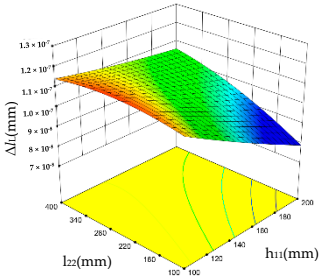

(**b**) Response surface relationship between structural deformation Δl_L and sensitive parameters l_{22} and h_{11}.

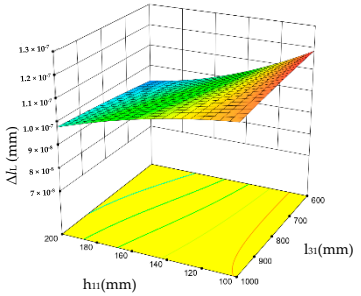

(**c**) Response surface relationship between structural deformation Δl_L and sensitive parameters l_{31} and h_{11}.

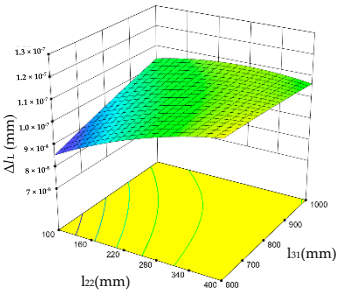

(**d**) Response surface relationship between structural deformation Δl_L and sensitive parameters l_{22} and l_{31}.

Figure 6. *Cont.*

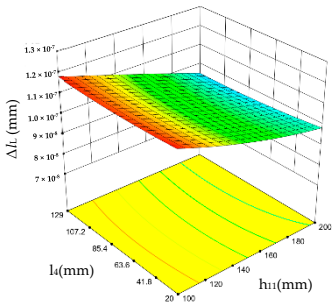

(**e**) Response surface relationship between structural deformation Δl_L and sensitive parameters l_4 and h_{11}.

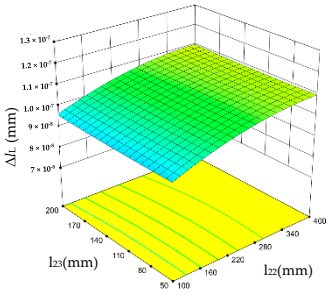

(**f**) Response surface relationship between structural deformation Δl_L and sensitive parameters l_{23} and l_{22}.

Figure 6. Response surface relationship between the deformation caused by thermal expansion Δl_L and sensitive parameters.

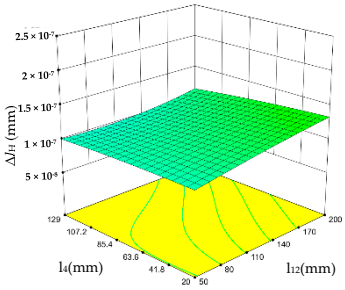

(**a**) Response surface relationship between structural deformation Δl_H and sensitive parameters l_{12} and l_4.

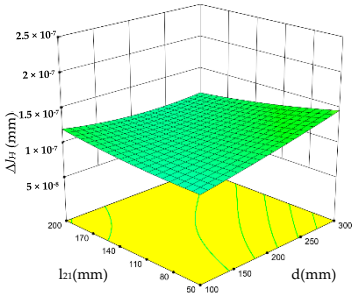

(**b**) Response surface relationship between structural deformation Δl_H and sensitive parameters l_{21} and d.

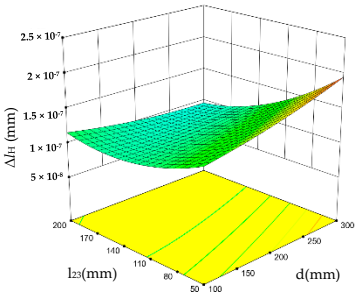

(**c**) Response surface relationship between structural deformation Δl_H and sensitive parameters l_{23} and d.

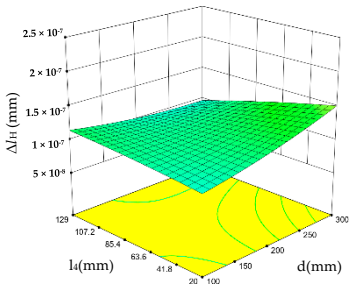

(**d**) Response surface relationship between structural deformation Δl_H and sensitive parameters l_4 and d.

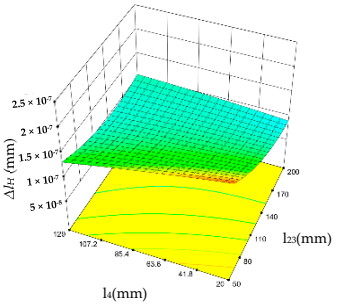

(**e**) Response surface relationship between structural deformation Δl_H and sensitive parameters l_4 and l_{23}.

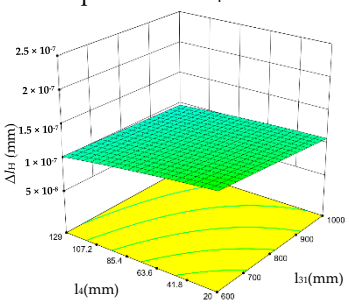

(**f**) Response surface relationship between structural deformation Δl_H and sensitive parameters l_4 and l_{31}.

Figure 7. Response surface relationship between the deformation caused by thermal expansion Δl_H and sensitive parameters.

Optimal parameters are computed using a search algorithm to satisfy minimum values of α_L and α_H, with a fundamental frequency greater than 50 Hz and a mass not exceeding 70 kg. Under the condition where the parameters of the core ultra-stable framework structure are set to their optimal values, the equivalent thermal expansion coefficients α_L and α_H in two in-plane directions are determined to be 8.3×10^{-8} and 7.0×10^{-8}, respectively. Based on the optimization results of the parameters, further optimization is conducted on the ultra-stable structural framework. Lightweight holes are appropriately machined in positions with minimal impact on the fundamental frequency to further reduce the overall weight of the ultra-stable structure. Additionally, diagonal reinforcements are added to positions with larger responses to enhance the structural resistance and mechanical properties of the framework. In order to verify whether the optimized structure can meet the requirements, HyperMesh is used to establish the finite element mesh model of the super-stable spacecraft structure framework. Since the main structural type of the main frame of the super-stable structure is the shell with different thicknesses, the shell element is established in the way of shell extraction during modeling, and the mesh size is 15 mm. The mesh model is shown in Figure 8. The finite element modeling software was used for pre-processing, The finite element analysis software was used for statical thermal deformation solution, and the maximum deformation of the structure under 1 K temperature load is 1.68×10^{-7} m. As shown in Figure 8, the equivalent thermal expansion coefficients α_L and α_H in two directions in the plane are 8.6×10^{-8}/K and 7.1×10^{-8}/K, respectively, indicating that the optimization results meet the requirement that the equivalent thermal expansion coefficient in the plane is less than 1×10^{-7}/K.

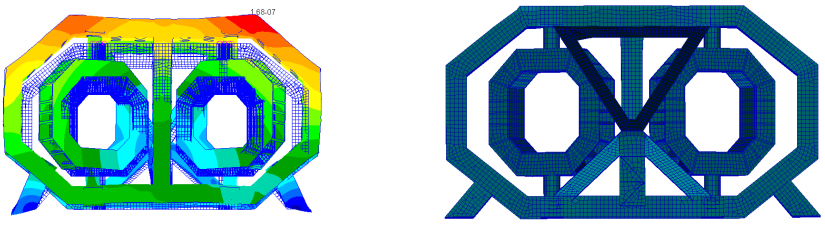

Figure 8. Finite element model of super-stable spacecraft structure.

6. Summary

This paper, based on the graded stability scheme of the gravitational-wave spacecraft, presents the indicator requirements for the core ultra-stable framework. The structural characteristics of the ultra-stable framework are analyzed, and a structural design scheme based on homogenized splicing of C/SiC box structures is proposed. Parameterized modeling and analysis of parameter constraint relationships for this topology structure are conducted. Combining the response surface method, a comprehensive parameter model linking framework design parameters with framework weight, strength, and temperature deformation is established. Ultimately, the optimal framework structure under the current state is obtained with overall dimensions of 1600 mm × 1300 mm × 110 mm, mass of 57.62 kg, and fundamental frequency of 54.3 Hz. The equivalent thermal expansion coefficients α_L and α_H in two directions are 8.6×10^{-8}/K and 7.1×10^{-8}/K, respectively. The results meet the requirements of weight less than 70 kg, fundamental frequency greater than 50 Hz, and linear expansion in two directions $\leq 1 \times 10^{-7}$/K, which proves that the multi-objective optimization method based on the response surface method is suitable for the optimal design of ultra-stable structures.

The design and manufacturing process of ultra-stable structural frameworks with minimal deformation are highly correlated, subject to more constraints, and require multi-objective optimization of optical, mechanical, thermal, and self-gravitational properties. Therefore, the material/structure/process collaborative design technology will be adopted in the future, and the coordinated integration of the design of the super-stable structure and the process will be realized through the multi-objective optimization method and topological complexity control technology. The ultra-stable structure with high stiffness and

light weight is designed. In the future, the C/SiC core super-stable frame of gravitational-wave spacecraft will be manufactured, and the thermal deformation test will be carried out by laser interferometer and high-precision vacuum thermal control system, and the parameter optimization results will be experimentally verified.

Author Contributions: Conceptualization, T.H., Z.X. and C.H.; methodology, K.H.; software, C.L.; validation, C.L. and K.H.; formal analysis, C.L.; resources, Z.X.; writing—original draft preparation, C.L.; writing—review and editing, C.L. and Z.X.; supervision, K.H.; project administration, C.L. All authors have read and agreed to the published version of the manuscript.

Funding: This work is supported by the National Key Research and Development Program of China [grant number 2022 YFC2204500].

Data Availability Statement: The data that support the findings of this study are available from the corresponding author, upon reasonable request.

Conflicts of Interest: The authors declare no conflict of interest.

References

1. Villalba, V.; Kuiper, H.; Gill, E. Review on thermal and mechanical challenges in the development of deployable space optics. *J. Astron. Telesc. Instrum. Syst.* **2020**, *6*, 010902. [CrossRef]
2. Shen, J.; Zhao, Y.; Liu, H.; Niu, Y.; Gao, R.; Guo, T.; Zhao, D.; Luo, Z. Multi-channel Thermal Deformation Interference Measurement of the Telescope Supporting Frame in Spaceborne Gravitational Wave Detection. *Microgravity Sci. Technol.* **2022**, *34*, 1–10. [CrossRef]
3. Ona, K.; Sakaguchi, N.; Ohno, H.; Utsunomiya, S. The Advanced Super Invar Alloys with Zero Thermal Expansion for Space Telescopes. *Trans. Jpn. Soc. Aeronaut. Space Sci. Aerosp. Technol. Jpn.* **2020**, *18*, 32–37. [CrossRef]
4. Hartmann, P.; Jedamzik, R.; Carré, A.; Krieg, J.; Westerhoff, T. Glass ceramic ZERODUR: Even closer to zero thermal expansion: A review, part 1. *J. Astron. Telesc. Instrum. Syst.* **2021**, *7*, 020901. [CrossRef]
5. Song, W. A Design of CFRP Supported Structure for a New Space Camera and Research on Mechanical and Thermal Stability of the Camera. Ph.D. Dissertation, Changchun Institute of Optics, Fine Mechanicsand Physics, University of Chinese Academy of Sciences, Beijing, China, 2022. [CrossRef]
6. Liu, J. Optimization Design and Performance Analysis of 3D Lattice Material with Zero-Expansion and High Ultra-Stiff. Ph.D. Dissertation, Dalian University of Technology, Dalian, China, 2020. [CrossRef]
7. Cao, X.; Yin, X.; Fan, X.; Cheng, L.; Zhang, L. Effect of PyC interphase thickness on mechanical behaviors of SiBC matrix modified C/SiC composites fabricated by reactive melt infiltration. *Carbon* **2014**, *77*, 886–895. [CrossRef]
8. Evans, J.S.O.; Hu, Z.; Jorgensen, J.D.; Argyriou, D.N.; Short, S.; Sleight, A.W. Compressibility, Phase Transitions, and Oxygen Migration in Zirconium Tungstate, ZrW_2O_8. *Science* **1997**, *275*, 61–65. [CrossRef] [PubMed]
9. Xiao, X.L.; Cheng, Y.Z.; Wu, M.M.; Peng, J.; Hu, Z.B. The study of thermal expansion properties in solid solutions Ln2−xCrxMo3O12 (Ln=Ho and Lu) by high temperature X-ray diffraction. *J. Phys. Chem. Solids* **2012**, *73*, 275–279. [CrossRef]
10. Goodman, W.A.; Nejhad, M.N.; Wright, S.; Welson, D. T300HoneySiC: A new near-zero CTE molded C/SiC material. *Int. Soc. Opt. Photonics* **2015**, *9574*, 110–115.
11. Zhang, K.; Wang, K.; Chen, J.; Wei, K.; Liang, B.; He, R. Design and additive manufacturing of 3D-architected ceramic metamaterials with programmable thermal expansion. *Addit. Manuf.* **2021**, *47*, 102338. [CrossRef]
12. Han, K.; Chen, L.; Xia, M.; Wu, Q.; Xu, Z.; Wang, G. Design and optimization of a high sensitivity joint torque sensor for robot fingers. *Measurement* **2020**, *152*, 107328. [CrossRef]
13. Chen, L.; Xuan, H.; Jia, W.; Liu, J.; Fang, Z.; Zheng, Y. Neck Structure Optimal Design of the Turbine Wheel for Containment Design of the Air Turbine Starter. *Aerospace* **2023**, *10*, 802. [CrossRef]
14. Duan, X.; Chang, J.; Chen, G.; Liu, T.; Ma, H. Contribution of Different Parameters on Film Cooling Efficiency Based on the Improved Orthogonal Experiment Method. *Aerospace* **2024**, *11*, 67. [CrossRef]
15. Lu, J.; Wang, J.; Lin, Y.; Zheng, K.; Tian, Z.; Han, P. The influence of particle surface oxidation treatment on microstructure and mechanical behavior of 3D-SiCp/A356 interpenetrating composites fabricated by pressure infiltration technique. *J. Mater. Res. Technol.* **2023**, *24*, 8984–8996. [CrossRef]
16. Schukraft, J.; Roßdeutscher, J.; Siegmund, F.; Weidenmann, K.A. Thermal expansion behavior and elevated temperature elastic properties of an interpenetrating metal/ceramic composite. *Thermochim. Acta* **2023**, *715*, 179298. [CrossRef]
17. Ivannikov, S.I.; Vahterova, Y.A.; Utkin, Y.A.; Sun, Y. Calculation of strength, rigidity, and stability of the aircraft fuselage frame made of composite materials. *INCAS Bull.* **2021**, *13*, 77–86. [CrossRef]